On the Stability and Convergence Rate of Some Discretized Schemes for Parametric Deformable Models Used in Medical Image Analysis

A.I. Mitrea[1], O.M. Gurzau[1], and P. Mitrea[2]

[1] Technical University of Cluj-Napoca, Dep. of Mathematics, Romania
[2] Technical University of Cluj-Napoca, Dep. of Computer Science, Romania

Abstract— **In order to find the energy-minimizing surface and to reduce the computational requirements, we consider an associated simplified model, [1], and we derive an algorithm for solving numerically the corresponding Euler-Gauss-Ostrogradsky equation of Calculus of Variations. The stability and the convergence of the algorithm are discussed, together with some aspects regarding the statistical modeling, applied in medical imaging.**

Keywords— **parametric deformable model, EGO-Equation, EGO-Algorithm, stability, convergence rate.**

I. INTRODUCTION

The theory of deformable models is an interdisciplinary scientific domain, which has appeared and developed in the last two decades, in strong connection with practical problems of medicine, image processing and physics; the deformable models represent a promising and vigorously researched model–based approach to computer–assisted medical image analysis.

Deformable models are viewed as curves or surfaces that can move under the influence of the internal forces, which are defined within the curve or surface itself, and external forces, which are computed from the image data [2],[3],[4].

Two basic type of deformable models were pointed out: the parametric or variational models and geometric models. The parametric models start from the original snake introduced by M. Kaas, A. Witkin and D. Terzopoulos [2] and represent curves and surfaces explicitly in their parametric form during the deformation process; the original snake was proposed as an interactive method, which requires expert guidance on the snake initialization and the selection of correct deformation parameters. In the last two decades, a set of deformable variational models have been proposed in order to improve the original snake, such as: *the balloon-snake model* of I. Cohen and L.D. Cohen [1], which add to the internal and external energies the so called balloon-energy and enables the initial contour to be located far from the desired boundary (the curve or surface is viewed as a balloon which is inflated); the *topology-snake* of T. Mc. Inerney and D. Terzopoulos [5], that designed a set of topology changing rules to be used during the balloon deformation; the *distance snake* of I. Cohen and L.D. Cohen [1], which is a deformation strategy implemented by means of the finite element method.

By means of some variational principles an energy-minimizing model (curve or surface) is achieved in this framework, by solving the Euler-Gauss-Ostrogradsky (EGO) Equation using discretized methods [1],[2],[6].

Regarding the geometric deformable models, we notice that these models were proposed independently by Cassels et al. [7] and Malladi et al. [8] and they are based on the curve evolution theory; in this framework the evolving models can be represented implicitly, as a level set of a higher-dimensional function [3,4].

This paper is concerned with the parametric deformable models; our goals are to derive an algorithm for obtaining the energy-minimizing surface, to establish its approximation error and to discuss the corresponding conditions of convergence and stability.

The paper outline is as follows. The next section defines the notion of deformable 3D-model and describes a method for obtaining a simplified 3D model as a sequence of plane curves. In the third section we point out an EGO-Algorithm of implicit type for the 3D simplified model. The convergence and the stability for an explicit-type discretized scheme derived from the algorithm of the third section are discussed in the fourth section. It must be mentioned that similar approaches regarding EGO-Algorithms and their approximation-error (but not their stability) can be found in [9]; however, the EGO-Algorithm presented in this paper is obtained in a different way, by using a general implicit discretization scheme and its convergence rate is better, because the inequalities involving the approximation-error are refined. The fifth section presents some aspects regarding the behavior of prosthetic surgical methods and prosthetic medical materials, based on Software tools, which implement the above mentioned mathematical methods.

II. ENERRGY MINIMIZING-SURFACES

From mathematical point of view, a 3D variational deformable model is emphasized by a family $\mathcal{A}$ of parameterized smooth surfaces with given boundary condition, named

S. Vlad and R.V. Ciupa (Eds.): MEDITECH 2011, IFMBE Proceedings 36, pp. 212–219, 2011.
www.springerlink.com

admissible surfaces, and an associated *energy-functional*. More exactly, let $D = [0,1] \times [0,1]$ be the unit square of $\mathbb{R}^2$ (or a compact plane domain) and

$$(S): \ v: D \to \mathbb{R}^3, \ v = v(s,r), \quad v = (x,y,z)^T; 0 \le s, r \le 1 \quad (1)$$

an arbitrary surface of class $C^2(D, \mathbb{R}^3)$ In this paper we use the notations $|v|^2 = x^2 + y^2 + z^2$, $v_s = \frac{\partial v}{\partial s}$, $v_r = \frac{\partial v}{\partial r}$, $v_{ss} = \frac{\partial^2 v}{\partial s^2}$, $v_{sr} = \frac{\partial^v}{\partial s \partial r}$, $v_{rr} = \frac{\partial^2 v}{\partial r^2}$. The family $\mathcal{A}$ of *admissible deformations* consists of all parameterized surfaces (1), subject to the boundary conditions $v(s,r) = g(s,r)$ and $\frac{\partial v}{\partial n}(s,r) = h(s,r)$ on the boundary ∂D of D, where $g \in C^2(\partial D, \mathbb{R}^3)$ and $h \in C^1(\partial D, \mathbb{R}^3)$ are given functions and n is the unit normal vector with respect to surface (1). Further, let us consider the following functions: the image intensity functions $I \in C^2(\mathbb{R}^3)$; *the potential function associated* to the external forces $P(v) = -\lambda |\nabla I(v)|^2$, $\lambda > 0$; *the control functions* corresponding to the internal forces acting on the shape of the surface, namely the elasticity functions $w_{10}(s;r)$and $w_{01}(s;r)$; the rigidity functions $w_{20}(s;r)$ and $w_{02}(s;r)$, and the *twist resistance function* $w_{11}(s;r)$.

The energy functional $E: \mathcal{A} \to \mathbb{R}$ incorporates the internal, external and balloon-energy, as follows:

$$E(v) = E_{int}(v) + E_{ext}(v) + E_{bal}(v)$$

$$\begin{gathered} E_{int}(v) = E_{els}(v) + E_{rig}(v) + E_{twr}(v) \quad (2) \\ E_{els}(v) = \iint_D \left(w_{10} |v_s|^2 + w_{01} |v_r|^2 \right) \mathrm{ds}\,\mathrm{dr} \\ E_{rig}(v) = \iint_D \left(w_{20} |v_{ss}|^2 + w_{02} |v_{rr}|^2 \right) \mathrm{ds}\,\mathrm{dr} \\ E_{twr}(v) = 2 \iint_D w_{11}(s,r) |v_{sr}|^2 \mathrm{ds}\,\mathrm{dr} \end{gathered}$$

$$E_{ext}(v) = \iint_D P(v(s,r))\, \mathrm{ds}\ \mathrm{dr} \quad (3)$$

$$E_{bal}(v) = \iint_D \det(c_0 v, v_s, v_r)\, \mathrm{ds}\,\mathrm{dr};\ c_0 > 0. \quad (4)$$

We notice that $E_{int}(v)$ represents *the internal energy*, $E_{ext}(v)$ is *the energy associated to the external forces* and $E_{bal}(v)$ is named *the balloon-energy*, which can be added, optionally, by the users (the term including $\det(c_0 v, v_s, v_r)$).

The triple $(\mathcal{A}, I, E)$ is said to be a *3D deformable model*, sometimes a *deformable surface*. The basic goal of a deformable model is to minimize its energy functional, which leads to the *energy-minimizing* surface, e.g. the optimal deformable model, provided by the Euler-Gauss-Ostrogradski (EGO) Equation of the Calculus of Variations:

$$\begin{gathered} \frac{\partial F}{\partial v} - \frac{\partial}{\partial s}\left(\frac{\partial F}{\partial v_s}\right) - \frac{\partial}{\partial r}\left(\frac{\partial F}{\partial v_r}\right) + \frac{\partial^2}{\partial s^2}\left(\frac{\partial F}{\partial v_{ss}}\right) + \\ + \frac{\partial^2}{\partial v \partial r}\left(\frac{\partial F}{\partial v_{sr}}\right) + \frac{\partial^2}{\partial r^2}\left(\frac{\partial F}{\partial v_{rr}}\right) = 0 \end{gathered} \quad (5)$$

together the Legendre-Sylvester minimum criterion.

Roughly speaking, the partial derivative (5) may have many solutions, so there may exist many local minimum energy-surfaces. But, in medical imaging the goal of the user is to find a good 3D-contour in a given area. Consequently, a rough prior estimate of the surface is provided (it is at hand of the user); further, this initial surface undergoes a deformation until reaching a local minimum of the energy-functional, according to (EGO) Equation (5). We achieve this deformation process by using the method of the Evolution Equation,[1].

Now, let us describe, mathematically, the method of Evolution Equation. Let

$$(S^0): v = v_0(s,r),\ (s,r) \in D \quad (6)$$

be an initial surface and denote by

$$(S^t): v = v(t,s,r);\ t \ge 0,\ (s,r) \in D \quad (7)$$

a family of surfaces, where the parameter $t \ge 0$ stands for the evolution in time of the model.

Denoting by $G(v, v_s, v_r, v_{ss}, v_{sr}, v_{rr})$ the left-hand member of (5), the *Evolution Equation* associated to the static model $(\mathcal{A}, I, E)$ is:

$$\frac{\partial v}{\partial t} + G(v, v_s, v_r, v_{ss}, v_{sr}, v_{rr}) = 0 \quad (8)$$

together with the initial estimate (condition)

$$v(0,s,r) = v_0(s,r),\ (s,r) \in D \quad (9)$$

and some boundary dynamic conditions.

A solution of the static problem is obtained when the solution $v(t,s,r)$ of (8) becomes stable, which means that $\frac{\partial v}{\partial t}$ approach to 0 (for $t \to \infty$) and the dynamic equation (8) reduces to the static equation (5)at infinity, see also [1].

However, the problem of finding the solutions of (EGO) Equation (8) is not practically possible, because these solutions contain long and complicated expressions or their explicit forms are inaccessible. On the other hand, by using discretized schemes for solving (8), we get a system of algebraic equations with a high computational level. These drawbacks are eliminated by passing to a 2D modeling problem, [1]. More exactly, the third component z of (S) is constrained to depend only on r, by setting $z(s,r) = r$. So, the surface that we seek is given as a sequence of plane curves, named *slices*, and the parameter r of (7) becomes the index of the corresponding slice. In this approach, the

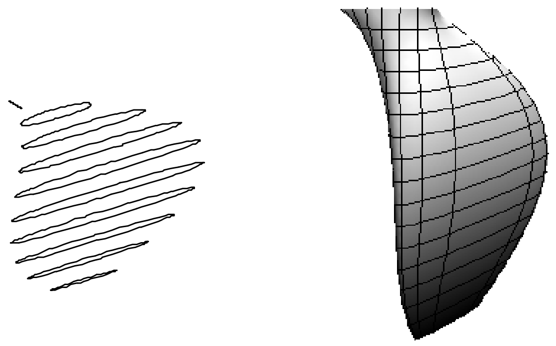

(a) (b)

Fig. 1 (a) Slices, (b) Surface

surface that we seek is viewed as a sequence of a planar curves (slices), indexed by the parameter r, so that each fixed value of r provides a closed curve, lying in a slice of the 3D-image. Consequently, let

$$(\gamma_r): v(s) = (x(s), y(s)),\ s \in [0,1] \tag{10}$$

be the 2D curve obtained by applying this reconstruction method, for a given r.

In what follows, we suppose that the control functions w_{ij} are positive constants and we set by the seek of simplicity, $w_1 = w_{10}$, $w_2 = w_{20}$. The (EGO) Equation (5), which corresponds to (γ_r), is:

$$2w_2\frac{d^4v}{ds^4} - 2w_1\frac{d^2v}{ds^2} - c_0J_2\frac{dv}{ds} + \nabla P = 0, \tag{11}$$

where $J_2 = \begin{bmatrix} 0 & 1 \\ -1 & 0 \end{bmatrix}$.

Example 1. If we consider in (11) $c_0 = -0.2$, $w_1 = 2.5$, $w_2 = 0.4$ $\quad P = r(x^2 + y^2)$ and $r = 0.1, 0.2, ..., 1$ with boundary conditions $x(0) = x(1) = 1 + \frac{r^2(1-r)^2}{25}$, $x'(0) = x'(1) = \frac{r(1-r)}{10}$, $y(0) = y(1) = 0 + \frac{r^2(1-r)}{25}$, $y'(0) = y'(1) = \frac{2r(1-r)}{5}$ we obtain the graphs of the slices and a 3D reconstruction of the surface, as it can be seen in the figure 1a and 1b.

III. An EGO-algorithm of implicit type for the 3D simplified model

Firstly, we use the method of finite differences in order to obtain the discretized version of the EGO-Equation , in dynamic form, see (8) and (11). Let δ and h be the time and the space discretization steps, respectively and denote the plane net of discretization by $\mathcal{R} = \{(t_k, s_i), k \geq 0,\ 0 \leq i \leq N\}$, with $N \in \mathbb{N}^*$, $Nh = 1$, $t_k = k\delta$ and $s_i = ih$. The following notations will be used, too: $v_i^k = v(t_k, s_i)$, $v^k = (v_i^k)_{0\leq k\leq N}$, $v^k = (x^k, y^k)$, $k \geq 0$, $g^k = (g_1^k, g_2^k)$, with $g_1^k = -\frac{1}{2}\left(\frac{\partial P}{\partial x}\right)(v^k)$, $g_2^k = -\frac{1}{2}\left(\frac{\partial P}{\partial y}\right)(v^k)$; since (γ_r) is a closed curve, it results $v_i^k = v_{i+N}^k$, $i \in \mathbb{Z}$. We approximate the partial derivatives at the nodes of $\mathcal{R}$ as follows:

$$\begin{cases} \frac{\partial v}{\partial t}(t_k, s_i) \simeq \frac{1}{\delta}\left(v_i^k - v_i^{k-1}\right); \frac{\partial v}{\partial s}(t_k, s_i) \simeq \frac{1}{h}\left(v_i^k - v_{i-1}^k\right) \\ \frac{\partial^2 v}{\partial s^2}(t_k, s_i) \simeq \frac{1}{h^2}\left(v_{i+1}^k - 2v_i^k + v_{i-1}^k\right) \\ \frac{\partial^4 v}{\partial s^4}(t_k, s_i) \simeq \frac{1}{h^4}\left(v_{i+2}^k - 4v_{i+1}^k + 6v_i^k - 4v_{i-1}^k + v_{i-2}^k\right) \end{cases} \tag{12}$$

with $k \geq 1; 0 \leq i \leq N$. With the notations $\gamma = \frac{c_0}{h}$, $a_1 = 2\frac{w_1}{h^2} + 6\frac{w_2}{h^4}$, $a_2 = -\frac{w_1}{h^2} - 4\frac{w_2}{h^4}$, $a_3 = \frac{w_2}{h^4}$, we consider the N-th order square matrices K (named *stiffness-matrix*) and L, defined as circular matrices with the first row $(a_1, a_2, a_3, 0, 0, \ldots, a_3, a_2)$ and $(1, -1, 0, 0, \ldots, 0)$, respectively. Thus, the differential equation (11) turns into the algebraic system

$$\frac{v^k - v^{k-1}}{\delta} + Kv^k + \gamma L\left(J_2v^k\right) = g^k, \quad k \geq 1. \tag{13}$$

Denote by $V^k = \left(X^k, Y^k\right)^T$, $k \geq 1$, the solution of the system (13), which approximate the values of $v(t,s)$ at the nodes of $\mathcal{R}$; these solutions satisfy the *discrete EGO-Equation* of implicit type

$$(I_N + \delta K)V^k + \delta\gamma L\left(J_2V^k\right) = V^{k-1} + \delta g^k,\ k \geq 1, \tag{14}$$

namely

$$\begin{cases} (I_N + \delta K)X^k + \delta\gamma LY^k = X^{k-1} + \delta g_1^k \\ (I_N + \delta K)Y^k - \delta\gamma LX^k = Y^{k-1} + \delta g_2^k \end{cases} : k \geq 1 \tag{15}$$

where I_N is the unit matrix of order N.

The equalities (14) and (15) define a totally implicit discretized scheme, since the unknown $V^k = \left(X^k, Y^k\right)^T$ appears in many terms of these relations (V^k is incorporated in g^k, too). Taking into account that g^k has a complicated expression (generally of non-linear type), we approximate the term g^k (which corresponds to the external forces) by its value of the previous iteration g^{k-1}, obtaining the following discretized scheme:

$$\frac{V^k - V^{k-1}}{\delta} + KV^k + \gamma L\left(J_2V^k\right) = g^{k-1} \tag{16}$$

The relation (16) defines a *semi-implicit discretized scheme*, because it is explicit with respect to the terms containing V^{k-1} and g^{k-1}, but it is implicit with respect to V^k.

Further, let us approximate both g^k and the matrix terms KV^k and $L\left(J_2V^k\right)$ of (14) by their values of the previous iteration, which leads to the *explicit discretized scheme* given by:

$$V^k=\left(I_N-\delta K-(\gamma\delta L)J_2\right)V^{k-1}+\delta g^{k-1}\ ;k\geq 1. \quad (17)$$

Remark that the EGO-Algorithm of explicit type (17) is a linear approximation of the corresponding implicit algorithms defined by (14) or (16).

Indeed, we derive from (14), with g^{k-1} instead of g^k, or from (16):

$$V^k=\left(I_N+\delta K\right)^{-1}\left(V^{k-1}+\delta g^{k-1}-\delta\gamma L\left(J_2V^{k-1}\right)\right)\quad k\geq 1. \quad (18)$$

On the other hand, from the matrix identity

$$\begin{aligned}&\left(I_N+\delta K\right)\left(I_N+\textstyle\sum_{j=1}^{m}(-1)^j\delta^jK^j\right)=\\&=I_N+(-1)^m\delta^{m+1}K^{m+1},\end{aligned} \quad (19)$$

it is easily seen that for $\delta\geq 0$ sufficiently small, by omitting the terms containing $\delta^m, m\geq 2$,the linear approximating formula

$$\left(I_N+\delta K\right)^{-1}\simeq I_N-\delta K \quad (20)$$

holds. Now, the relations (18) and (20) lead to (17).

IV. THE CONVERGENCE AND THE STBILITY OF THE EXPLICIT EGO-ALGORITHM

In this section we refer to the explicit EGO-Algorithm (17). Setting $\alpha=\frac{w_1}{h^2}$ and $\beta=\frac{w_2}{h^4}=a_3$, we derive from (17):

$$\begin{aligned}V_i^k=&-\beta\delta V_{i+2}^{k-1}+\delta\left(\left(\alpha+4\beta\right)I_2+\gamma J_2\right)V_{i+1}^{k-1}+\\&+\left(\left(1-2\alpha\delta-6\beta\delta\right)I_2-\gamma\delta J_2\right)V_i^{k-1}+\\&+\delta\left(\alpha+4\beta\right)V_{i-1}^{k-1}-\beta\delta V_{i-2}^{k-1}+\delta g_i^{k-1},\\&k\geq 1, 0\leq i\leq N-1\end{aligned} \quad (21)$$

with $V_i^k=\left(X_i^k,Y_i^k\right)^T$, $V_j^k=V_{j+N}^k,\ j\in\mathbb{Z},\ k\geq 0$ and $g_i^k=\left(g_{1i}^k,g_{2i}^k\right)$, $g_{1i}^k=-\frac{1}{2}\frac{\partial P}{\partial x}\left(v_i^k\right)$, $g_{2i}^k=-\frac{1}{2}\frac{\partial P}{\partial y}\left(v_i^k\right)$.

In order to establish the convergence of the EGO-Algorithm (21), denote by

$$\varepsilon_i^k=v_i^k-V_i^k,\ k\geq 0,\ 0\leq i\leq N-1 \quad (22)$$

By using the Taylor expansions of $v(t,s)$ at the point $N_i^{k-1}(t_{k-1},s_i)\in\mathcal{R}$, namely:

$$\begin{cases}v_i^k=v_i^{k-1}+\delta\frac{\partial v}{\partial t}\left(N_i^{k-1}\right)+\frac{\delta^2}{2!}\frac{\partial^2 v}{\partial t^2}\left(N_i^{k-1}\right)+\cdots\\ v_{i\pm1}^{k-1}=v_i^{k-1}\pm h\frac{\partial v}{\partial s}\left(N_i^{k-1}\right)+\\ +\frac{h^2}{2!}\frac{\partial^2 v}{\partial s^2}\left(N_i^{k-1}\right)\pm\frac{h^3}{3!}\frac{\partial^3 v}{\partial s^3}\left(N_i^{k-1}\right)+\cdots\\ v_{i\pm2}^{k-1}=v_i^{k-1}\pm 2h\frac{\partial v}{\partial s}\left(N_i^{k-1}\right)+\\ +\frac{(2h)^2}{2!}\frac{\partial^2 v}{\partial s^2}\left(N_i^{k-1}\right)\pm\frac{(2h)^3}{3!}\frac{\partial^3 v}{\partial s^3}\left(N_i^{k-1}\right)+\cdots\end{cases} \quad (23)$$

we obtain from (21), (22) , (23):

$$\begin{aligned}\varepsilon_i^k=&\left(\left(1-2\alpha\delta-6\beta\delta\right)I_2-\gamma\delta J_2\right)\varepsilon_i^{k-1}+\\&+\delta\left(\left(\alpha+4\beta\right)I_2+\gamma J_2\right)\varepsilon_{i+1}^{k-1}+\\&+\delta\left(\alpha+4\beta\right)\varepsilon_{i-1}^{k-1}-\beta\delta\left(\varepsilon_{i+2}^{k-1}+\varepsilon_{i-2}^{k-1}\right)+\delta Rv_i^{k-1},\end{aligned} \quad (24)$$

where Rv_i^{k-1} is the *residue* of the algorithm, see [10], namely:

$$\begin{aligned}Rv_i^{k-1}=&\ \delta\left(\frac{1}{2}\frac{\partial^2 v}{\partial t^2}+\frac{1}{6}\delta\frac{\partial^3 v}{\partial t^3}+\cdots\right)\left(N_i^{k-1}\right)+\\&+h^2w_2\left(\frac{1}{6}\frac{\partial^6 v}{\partial s^6}+\frac{127}{5040}h^2\frac{\partial^8 v}{\partial s^8}+\cdots\right)\left(N_i^{k-1}\right)-\\&-w_1h^2\left(\frac{1}{12}\frac{\partial^4}{\partial s^4}+\frac{h^2}{60}\frac{\partial^6 v}{\partial s^6}+\cdots\right)\left(N_i^{k-1}\right)-\\&-c_0J_2h\left(\frac{1}{2}\frac{\partial^2 v}{\partial s^2}+\frac{h^2}{24}\frac{\partial^4 v}{\partial s^4}+\cdots\right)\left(N_i^{k-1}\right);\\&0\leq i\leq N-1;k\geq 1\end{aligned} \quad (25)$$

Let

$$E^k=\max\left\{|\varepsilon_{i\pm2}^k|,|\varepsilon_{i\pm1}^k|,|\varepsilon_i^k|,0\leq i\leq N-1\right\},k\geq 0 \quad (26)$$

the *approximation-error* at the *k*-th iteration of the EGO-Algorithm. Suppose that the partial derivatives in (25) are uniformly bounded. Thus, the relations (24), (25) and (26), combined with the classical inequality $\sqrt{x^2+y^2}\leq|x|+|y|, x,y\in\mathbb{R}$, provides the upper estimate:

$$\begin{aligned}E^k\leq&\left(10\beta\delta+2\alpha\delta+2\gamma\delta+\left(1-2\alpha\delta-6\beta\delta\right)\right)E^{k-1}+\\&+M_1\delta^2+M_2|2w_2-w_1|\delta h^2+M_3c_0\delta h\end{aligned} \quad (27)$$

Under the practical assumption (in medical imaging, for example)

$$1-6\beta\delta-2\alpha\delta>0 \quad (28)$$

we derive from (27):

$$E^k\leq qE^{k-1}+M_1\delta^2+M_2|2w_2-w_1|\delta h^2+M_3c_0\delta h \quad (29)$$

for $k\geq 1$, with:

$$q=1+4\beta\delta+2\gamma\delta \quad (30)$$

Writing the estimate (29), successively, for $k, k-1, \ldots, 1$ and taking into account that $E^0 = 0$, we get:

$$E^k \le \frac{q^k - 1}{q - 1} \cdot M(h, \delta), \tag{31}$$

with

$$M(h, \delta) = M_1 \delta^2 + M_2 |2w_2 - w_1| \delta h^2 + M_3 c_0 \delta h \tag{32}$$

Now, from the previous notations, we get:

$$w_1 = \alpha h^2, \; w_2 = \beta h^2 \text{ and } c_0 = \gamma h \tag{33}$$

In the medical imaging the parameters α, β and γ are viewed as absolutely positive constants, [1], what is in accordance with the hypothesis (28) written in the form:

$$\delta < \frac{1}{6\beta + 2\alpha}, \tag{34}$$

The inequalities $1 + 4\beta\delta \le q \le 1 + 6\beta\delta$, which follows from (30) and (33), combined with the relations (31), (32) and $(1+x)^{1/x} \le e$ for $x > 0$, lead to the estimate:

$$\begin{aligned} E^k \le \tfrac{\exp(6\beta\delta k) - 1}{4\beta} \cdot \\ \cdot \left(M_1 \delta + M_2 |2\beta h^2 - \alpha| h^4 + M_3 \gamma h^2 \right) \end{aligned} \tag{35}$$

With the practical hypothesis:

$$k\delta = O(1) \tag{36}$$

we derive from (35), for $h > 0$ sufficiently small and $\delta = O\left(\frac{1}{k}\right)$

$$E^k = \begin{cases} O(\delta) + O(h^2), \text{ if } c_0 > 0 \\ O(\delta) + O(h^4), \text{ if } c_0 = \gamma = 0 \end{cases} \tag{37}$$

It is easily seen that (36) implies (34) for k sufficiently large. Therefore, $E^k \to 0$ if $\delta \to 0, h \to 0$, so that the following convergence statement holds.

If the condition (36) is fulfilled and the weight-coefficients w_1, w_2 and c_0 are given by (33), then the EGO-Algorithm (21) is convergent and its approximation-error at the k-th iteration satisfies the estimate (37).

Further, let us examine *the stability of the explicit EGO-Algorithm* (21), with $c_0 = 0$, i.e. $\gamma = 0$. The intuitive idea regarding the stability is that small errors in the initial conditions should cause small errors in the solution. On the other hand, the study of the stability is necessary in order to use the Lax Theorem of convergence [11]. By omitting the small term $\delta R v_i^{k-1}$ in (24), the errors $\tilde{\varepsilon}_i^k$ of the EGO-Algorithm (21) with $c_0 = \gamma = 0$ satisfy the relation:

$$\begin{aligned} \tilde{\varepsilon}_i^k = (1 - 6\beta\delta - 2\alpha\delta)\, \tilde{\varepsilon}_i^{k-1} + \\ (\alpha\delta + 4\beta\delta) \left(\tilde{\varepsilon}_{i+1}^{k-1} + \tilde{\varepsilon}_{i-1}^{k-1} \right) - \\ -\beta\delta \left(\tilde{\varepsilon}_{i+2}^{k-1} + \tilde{\varepsilon}_{i-2}^{k-1} \right), k \ge 1 \end{aligned} \tag{38}$$

In order to use the method of von Neumann [10,12],let

$$\begin{aligned} \tilde{\varepsilon}_i^k = \exp(\mu k \delta) \cdot \exp(j\omega i h) \cdot (1,1)^T = \\ = \mu^k \cdot \exp(j\omega i h)(1,1)^T, \mu = \exp(\nu\delta) \end{aligned} \tag{39}$$

where j and $\nu = \nu(\omega)$ are complex number, $j^2 = -1$ and ω denotes the frequency. Taking into account that $|exp(j\omega ih)| = 1$, it is obvious that the error $\tilde{\varepsilon}_i^k$ doesn't increase in time if

$$|\mu| < 1. \tag{40}$$

The inequality (40) is referred to as the *stability criterion of von Neumann*.

In our case, we derive from (38) and (39) with $\eta = \omega h$

$$\begin{aligned} \mu = (1 - \alpha\delta - 6\beta\delta) + \\ +\delta(\alpha + 4\beta)(\exp(j\eta) + \exp(-j\eta)) - \\ -\beta\delta(\exp(2j\eta) + \exp(-2j\eta)) \end{aligned} \tag{41}$$

By using the relations $\exp(j\alpha) + \exp(-j\alpha) = 2\cos\alpha$ and $1 - \cos\alpha = 2\sin^2(\alpha/2), \alpha \in \mathbb{R}$ the equality (41) becomes:

$$\mu = 1 - 4\alpha\delta \sin^2\eta - 16\beta\delta \sin^4\eta \tag{42}$$

Now, combining the relations (40) and (42) we get:

$$2\alpha\delta + 6\beta\delta \le 1. \tag{43}$$

namely

$$2\frac{\delta}{h^4}\left(w_1 h^2 + 4w_2\right) \le 1, \tag{44}$$

which represents *the stability condition* of the considered EGO-Algorithm. Remark that the inequality (44) leads to the *necessary stability conditions*:

$$w_2 \frac{\delta}{h^4} \le \frac{1}{8}; \quad w_1 \frac{\delta}{h^2} \le \frac{1}{2} \tag{45}$$

V. MONITORING THE BEHAVIOR OF PROSTHETIC SURGICAL METHODS AND PROSTHETIC MEDICAL MATERIALS, BASED ON SOFTWARE IMPLEMENTATION

In order to apply the results of the theoretical researches detailed above in the medical imaging domain, a 3D visual software environment –named MoDef- was implemented, aiming to visualize and follow-up the deformation behavior of the surgical (abdominal, maxilla-facial and orthodontic) prosthetic materials. That is performed on three distinct, but convergent levels, as follows:

a) 3d reconstruction visual software component, aimed to tracks the evolution of the prosthetic materials, based on processing the US images of the anatomic context of a lot of surgical patients;

b) deformable prosthetic material's behavior forecasting software component, based on software tools which implements the above described mathematical methods;

c) comparative parallel tracking software component, aimed to simultaneous supervise in time both (a) and (b) levels, in comparison with the results provided by the stochastic analysis component of the 3D visual software environment MoDef.

Concerning the 3D visualizing of the prosthetic meshes by means of the MoDef software environment components, two levels of reconstruction are performed, namely:

1) On the first level, a polynomial interpolation method is applied on each slice of the US image of the prosthetic mesh, acquired based on succeeding positions of the transducer, obtained by rotating them with a constant angle in a same pre-established direction; more exactly, the curves representing the sections of the surgical mesh acquired by the transducer, are extracted from the context of the US image, based on specific image processing methods - namely contour detection methods, that are implemented at the level of the image processing operators of the MoDef environment's image processing library. Starting with this set of basic mesh surface definition curves, extracted from the US images acquired at pre-established moments in time, a complete and consistent collection of 3D generator curve sets is obtained, by means of 3D polynomial interpolation methods, based on Lagrange, Hermite or Birkhoff operators.

2) On the second level, the complete collection of the 3D generator curves obtained at the first level is processed based on Blended Interpolating Methods (BIM), as well as with 3D continuous representation techniques, in order to obtain "solid-view", respectively "wired-view" representations of the prosthetic mesh.

In what follows some preliminary experiments made in 3DS Max7, followed by some relevant results obtained with the 3D Reconstruction component of MoDef 3D Visual environment are presented.

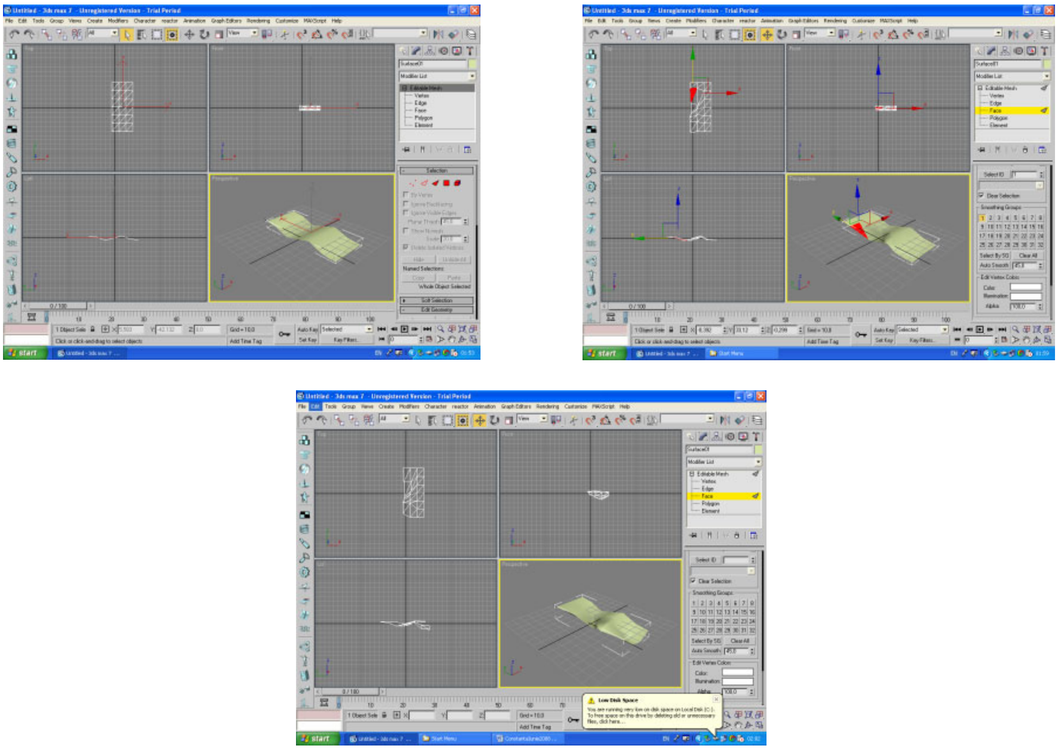

Fig. 2 Preliminary experiments made in 3DS Max7

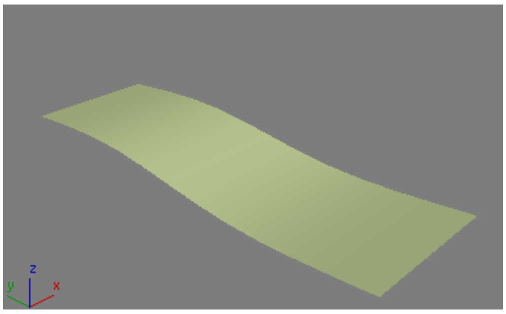

(a) Initial 3D representation of the deformable surface of the surgical mesh

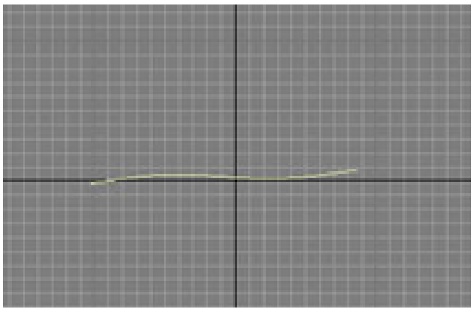

(b) Curve representing a section of the surgical mesh acquired by the transducer, extracted from the context of the US image based on specific image processing methods

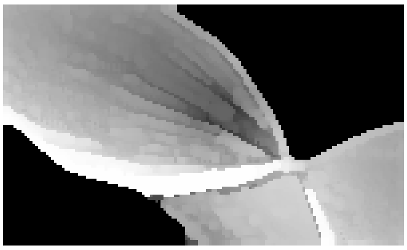

(c) The surface of the prosthetic mesh after the deformations produced in time due to the anatomic assimilation process

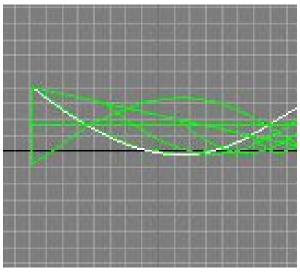

(d) The basic set of generating curves, used to obtain the “solid-view” representations of the prosthetic mesh

Fig. 3 Results obtained with the 3D Reconstruction component of MoDef 3D Visual environment

VI. Conclusions

In this paper we considered a 3D parametric deformable model and we defined, according to [1], its associated simplified model, with the aim to reduce the computational requirements. In order to find the energy-minimizing surface (the optimal model), we derived an EGO-Algorithm of implicit type, starting from the EGO-Equation of Calculus of Variations and using a finite difference method. We estimate the approximation error of this algorithm and we established conditions of its convergence and stability. Some considerations about the statistical modeling were presented, too. Our next target consists in using the discretized scheme of Krank-Nicolson and finite-element methods in order to obtain new results concerning the rate of convergence and the stability of the corresponding algorithms; the probabilistic and geometric deformable models will be considered, too, in our approaches.

Acknowledgment

These researches are supported by the Project PN2-Partnership, No. 11018 (MoDef).

References

1. L.D. Cohen and I. Cohen. (1993). Finite Element Methods for Active Contour Models and Balloons for 2D and 3D Images. IEEE PAMI 15(11), 1131—1150.
2. Michael Kaas, Andrew Witkin, and Demetri Terzopoulos. (1988) Snakes: Active contour models. International Journal of Computer Visison 1, 321—331.
3. L.He, Zh.Pens, B.Guarding, X.Wang, C.Y.Han, K.L.Weiss and W. G. Wer (2008) A comparative study of deformable contour methods on medical image segmentation Image and Comp.Vision, 26, 141-163.
4. R.Hegadi, A. Kop, M. Hangarge (2010) A Survey on Deformable Model and its Applications to Medical Imaging, IJCA Special Issue on “Recent trends in Image Processing and Pattern Recognition.
5. T. McInerney, D. terzopoulos (2000), T-snakes:topologically adaptive snakes,Med. Image Analysis, 4(2),73-91

6. S. Nedevschi and D. Mitrea. (2003) Contour detection based on active contour models. Bull.Appl.Math.Comp.Sci. (Techn. Univ. of Budapest) XCVII(2275), 107—118.
7. V. Caselles, F. Catte, T. Coll, and F.Dibos. (1993).A geometric model for active contours. Numerische Mathematik 66, 1—31.
8. R. Malladi, J. Sethian, and B. Vemuri. (1995) Shape modeling with front propagation: A level set approach. PAMI 17(2), 158—175.
9. A.I.Mitrea, O.M.Gurzau, P.Mitrea, D.Cimpean, Numerical methods for finding the optimal model in the theory of deformable models, Proceedings of 12-th Symposium of Mathematics and its Applications, Ed. Politehnica, Timisoara(2009), pp.446-453, ISSN 1224-6069
10. D. Trif. (1997). Numerical methods for differential equations (in romanian) Ed. Transilvania Press .
11. G. Aubert, P. Kornprobst (2006) Mathematical Problems in Image Processing. Partial Differential Equations and the Calculus of Variations, Springer
12. E.Isaacson , B. Keller, (1966) Analysis of Numerical Methods, New York, Wiley and Sons.

Author: Alexandru Ioan Mitrea
Institute: Technical University of Cluj-Napoca
Street: G. Baritiu 25
City: Cluj-Napoca
Country: Romania
Email: Alexandru.Ioan.Mitrea@math.utcluj.ro